ACS NANO

www.acsnano.org

ARTICLE

Optical Imaging of a Single Molecule with Subnanometer Resolution by Photoinduced Force Microscopy

Tatsuya Yamamoto, Hidemasa Yamane, Nobuhiko Yokoshi, Hisaki Oka, Hajime Ishihara,* and Yasuhiro Sugawara*

Cite This: *ACS Nano* 2024, 18, 1724−1732

Read Online

ACCESS | Metrics & More | Article Recommendations | Supporting Information

ABSTRACT: **Visualizing the optical response of individual molecules is a long-standing goal in catalysis, molecular nanotechnology, and biotechnology. The molecular response is dominated not only by the electronic states in their isolated environment but also by neighboring molecules and the substrate. Information about the transfer of energy and charge in real environments is essential for the design of the desired molecular functions. However, visualizing these factors with spatial resolution beyond the molecular scale has been challenging. Here, by combining photoinduced force microscopy and Kelvin probe force microscopy, we have mapped the photoinduced force in a pentacene bilayer with a spatial resolution of 0.6 nm and observed its "multipole excitation". We identified the excitation as the result of energy and charge transfer between the molecules and to the Ag substrate. These findings can be achieved only by combining microscopy techniques to simultaneously visualize the optical response of the molecules and the charge transfer between the neighboring environments. Our approach and findings provide insights into designing molecular functions by considering the optical response at each step of layering molecules.**

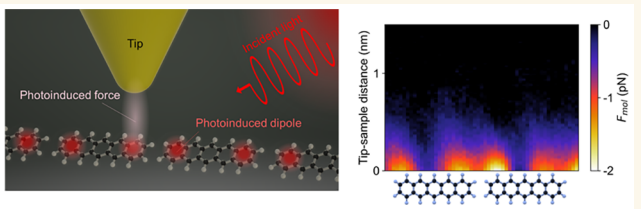

KEYWORDS: *optical imaging, single molecule, photoinduced force microscopy, PiFM, NC-AFM, KPFM*

Visualizing the optical response of individual molecules at the molecular scale is a challenging task and a long-standing goal in catalysis,[1] molecular nanotechnology,[2] and biotechnology.[3] The optical response of molecules is dominated by not only the electronic states in their isolated environment but also by the neighboring molecules. When the intermolecular distance is very small, charge transfer occurs because of the mixing of wave functions of molecules.[4] In addition, for charge transfer to occur, the molecular orbitals of the molecule donating the charge and the molecule accepting the charge must have an appropriate energy relationship.[5] Thus, the intermolecular distance, the relationship between the energies of the molecular orbitals, and the charge transfer between molecules are very important factors in studying the details of the optical response of molecules. So far, studies on the optical response of molecules above the molecular scale have been reported, including those on the mapping of vibrations[6−8] and the properties of excited states.[9,10]

Recently, an optical microscopy concept (photoinduced force microscopy: PiFM) (Figure 1a), which detects the intensity distribution of near-field light localized on a material surface as a force, has attracted much attention as a method to study the local optical response of materials.[11−14] The dipole−dipole interaction between the dipole induced by the tip and the dipole induced by the sample surface is measured as a photoinduced force[12] (see Supplementary Notes 1 and 2). The local optical responses of materials can be visualized with high spatial resolution[14] because the photoinduced force is inversely proportional to the fourth power of the tip−sample distance (see Supplementary Notes 3 and 4). Various optical responses have been investigated by PiFM, including nanoscale linear and nonlinear optical responses,[15] the Raman effect,[16] and optical and mechanical molecular damping.[17] Since PiFM is based on atomic force microscopy (AFM), the structure of the sample surface, including insulator surfaces, can be observed, and the charge transfer (or change in the contact potential difference (CPD)) of the sample can be measured by using Kelvin probe force microscopy (KPFM).[18,19] PiFM is an ideal

Received: November 5, 2023
Revised: December 22, 2023
Accepted: December 26, 2023
Published: December 29, 2023

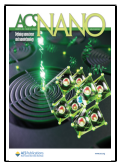

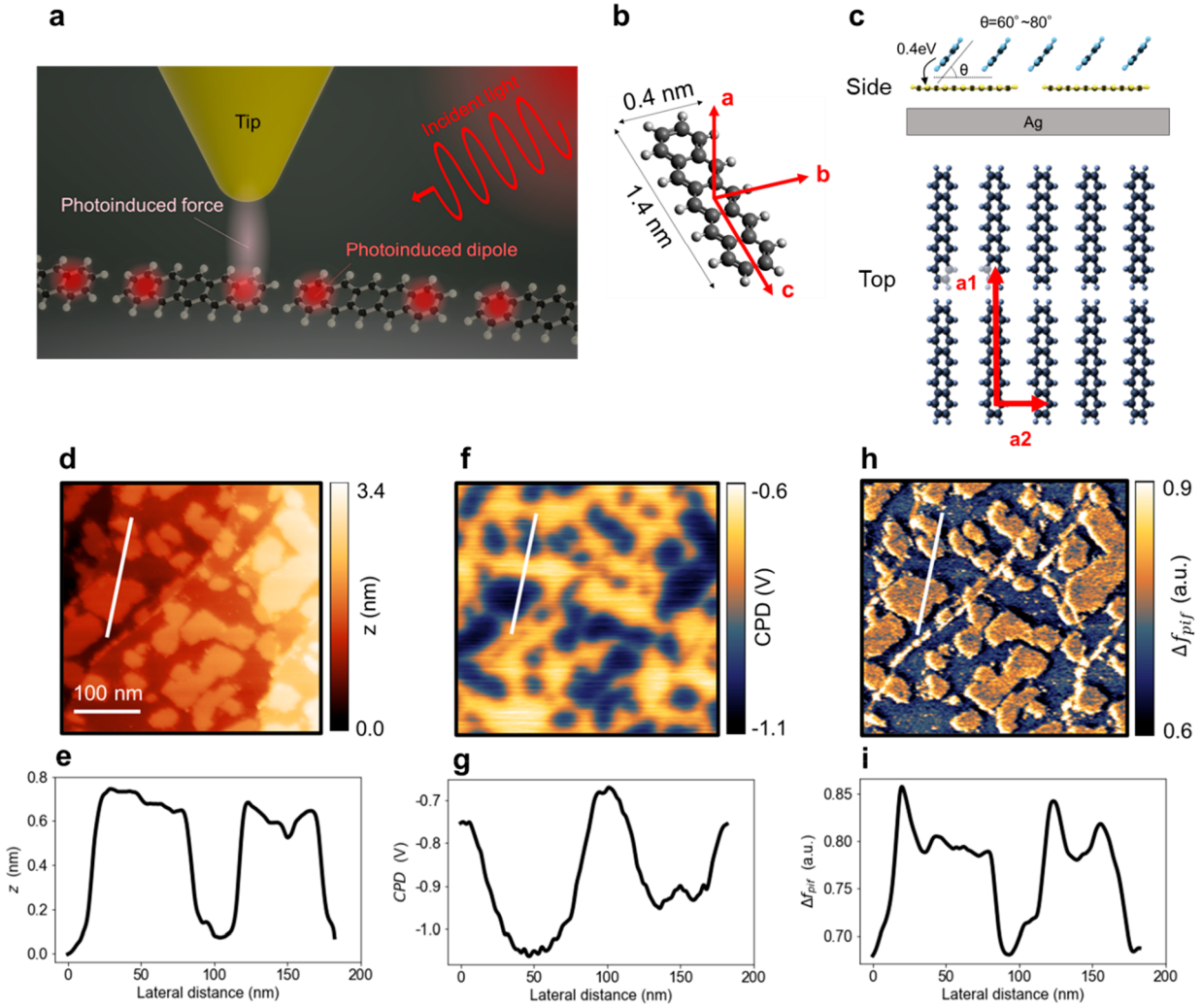

Figure 1. Configuration of the PiFM instrument and the PiFM measurement of a pentacene thin film. (a) Schematic diagram of PiFM under ultrahigh vacuum (UHV) and low temperatures with a side-illumination configuration of the incident light. The dipole−dipole interaction between the photoinduced dipoles on the tip and the sample is detected as a "photoinduced force". (b) Atomic structure of the pentacene molecule. (c) Molecular arrangement of the pentacene bilayer on the Ag (100) surface. The pentacene monolayer is flatly adsorbed on the Ag surface, while upper-layer molecules of the pentacene bilayer are adsorbed on the lower-layer molecules at an angle of 60−80 degrees around the *c* axis (b). (d, e) Topography of the pentacene thin film on Ag (100) and its line profile: A pentacene bilayer is formed as islands, and a pentacene monolayer covers the rest of the surface. (f, g) CPD image and its line profile; (h, i) PiFM (Δf_{pif}) image and its line profile. A laser beam with a wavelength of 690 nm is incident from the right side. (d)−(h) were simultaneously obtained at Δf = −110 Hz (tip−molecule spacing of 0.9 nm).

experimental platform for studying the optical response of materials at the nanoscale, which has not been previously investigated in detail.

Here, we investigate the optical response of a single pentacene molecule (Figure 1b) using PiFM based on the heterodyne frequency modulation (heterodyne FM) method[20,21] and KPFM. The optical response inside the single molecule where charge transfer occurred was successfully observed with a spatial resolution of 0.6 nm, and the multipole excitation of the single molecule was visualized. The two-dimensional (2D) mapping of the photoinduced forces revealed that the signal is strong at the edges of the molecule and is almost absent in the center. Theoretical calculations show that when no charge transfer occurs, the perpendicular components of the dipole are strongly excited at the center of the molecule, whereas when charge transfer occurs, the perpendicular components of the dipole are strongly excited at the edge of the molecule and cancel out at the center. This result is a real-space visualization of the optical response of a single molecule highly affected by charge transfer, which could not be observed by conventional methods.

RESULTS AND DISCUSSION

Figures 1d, 1e, and 1f show the topographic, CPD, and PiFM images simultaneously measured for a pentacene thin film on a Ag (100) substrate. Laser light with a wavelength of 690 nm was incident from the side of the probe on the pentacene thin film on the Ag substrate at an angle of 70° to the substrate normal. The power of the laser light was 7 mW, and the radius of the laser spot at the tip was 1.4 μm. From the topography in Figure 1d, we can see that a pentacene bilayer is formed as islands and that a pentacene monolayer covers the rest of the surface.[22,23] The height difference between the pentacene bilayer and the pentacene monolayer is 550−600 pm, indicating that the upper-layer molecules were adsorbed on

https://doi.org/10.1021/acsnano.3c10924
ACS Nano 2024, 18, 1724−1732

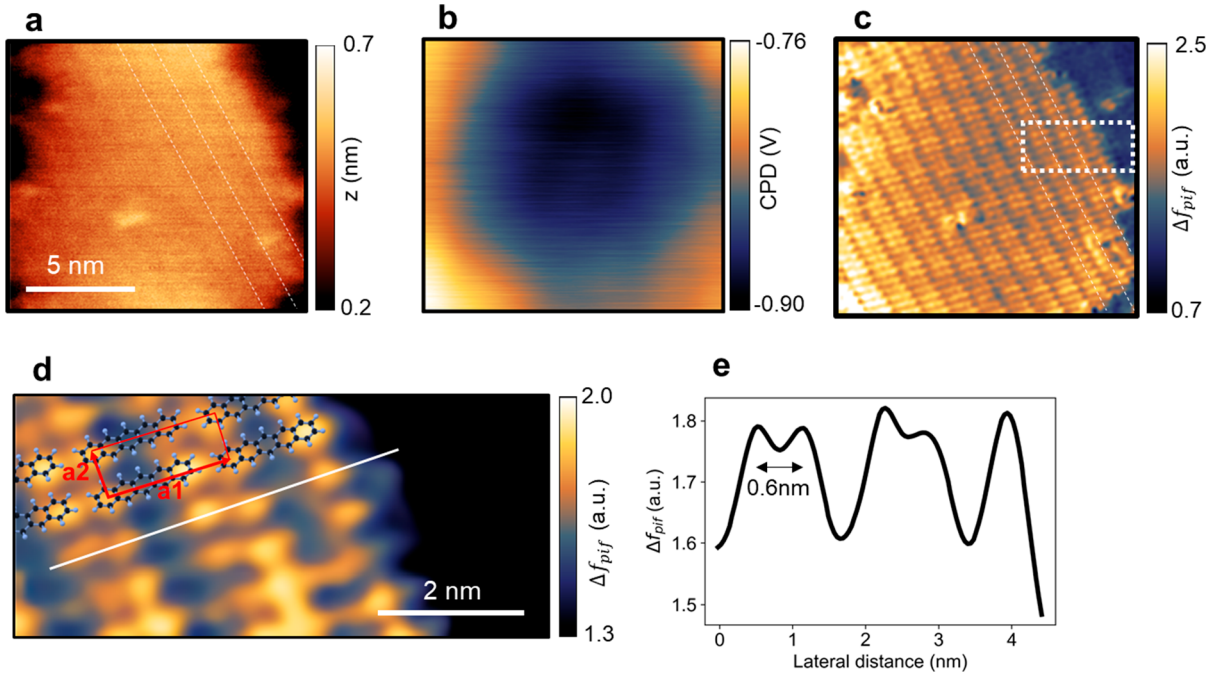

Figure 2. Photoinduced force mapping with submolecular resolution on a pentacene bilayer. (a) Topographic, (b) CPD, and (c) PiFM (Δf_{pif}) images of a pentacene bilayer. (d) Enlarged PiFM image with submolecular resolution of the area indicated by the dashed white square in (c). (e) Line profile along the white line in (d). (a)−(d) were simultaneously obtained at $\Delta f = -160$ Hz (tip−molecule spacing of 0.4 nm).

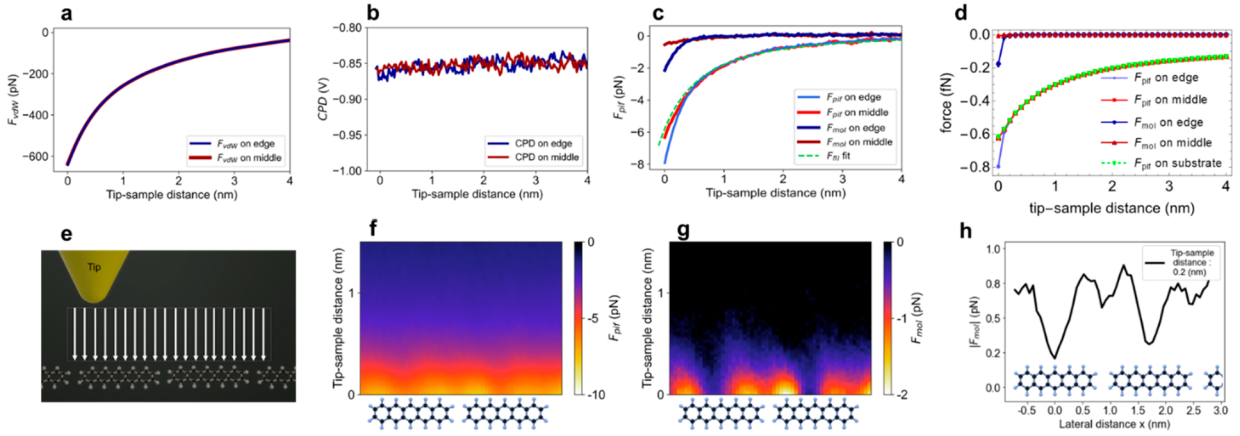

Figure 3. Force curves and 2D photoinduced force mapping with submolecular resolution of a pentacene bilayer. (a) Force curves of the van der Waals force, (b) *z*-spectroscopy of CPD, and (c) force curves of photoinduced force measured on the edge and on the middle of a single pentacene molecule. (d) Calculated curves of photoinduced force at the edge and in the middle of a single pentacene molecule. (e) Graphical model of 2D mapping of photoinduced force F_{pif}. (f) 2D mapping result of photoinduced force F_{pif}. (g) 2D mapping result of short-range photoinduced force F_{mol}. (h) Profile of short-range photoinduced force F_{mol} at the tip−sample distance z = 0.2 nm in (g).

the lower-layer molecules at an angle of 60−80 degrees to the Ag surface (Figure 1c).[22,23] From the CPD image in Figure 1f, we can see that there is a CPD between the pentacene bilayer and the pentacene monolayer. The CPD of the pentacene bilayer was approximately 0.4 V smaller than that of the pentacene monolayer (Figures 1f and 1g). A study previously showed that when pentacene molecules are adsorbed on a Ag surface, they donate negative charges to the Ag surface, resulting in the generation of upward-interface dipoles at the pentacene/Ag junction.[24] The experimental results in Figures 1f and 1g suggest that more electrons are transferred from the upper-layer molecules to the Ag substrate side than from the lower-layer molecules, resulting in larger interfacial dipoles. In the PiFM images in Figures 1h and 1i, high contrast appears between the pentacene monolayer and the pentacene bilayer: the photoinduced force of the pentacene bilayer is greater than that of the pentacene monolayer. In the PiFM image, artifacts derived from the electrostatic forces (CPD) acting between the tip and the pentacene film are removed (see Supplementary Note 8 for the photoinduced force enhancement at the left edge of the bilayer islands and Supplementary Notes 4, 9, and 10 for the removal of artifacts).

Next, we performed PiFM imaging of a pentacene bilayer with the tip 0.5 nm closer to the sample than that in Figure 1. In Figures 2a, 2b, and 2c, we show the topographic, CPD, and PiFM (Δf_{pif}) images simultaneously measured for the

https://doi.org/10.1021/acsnano.3c10924
ACS Nano 2024, 18, 1724−1732

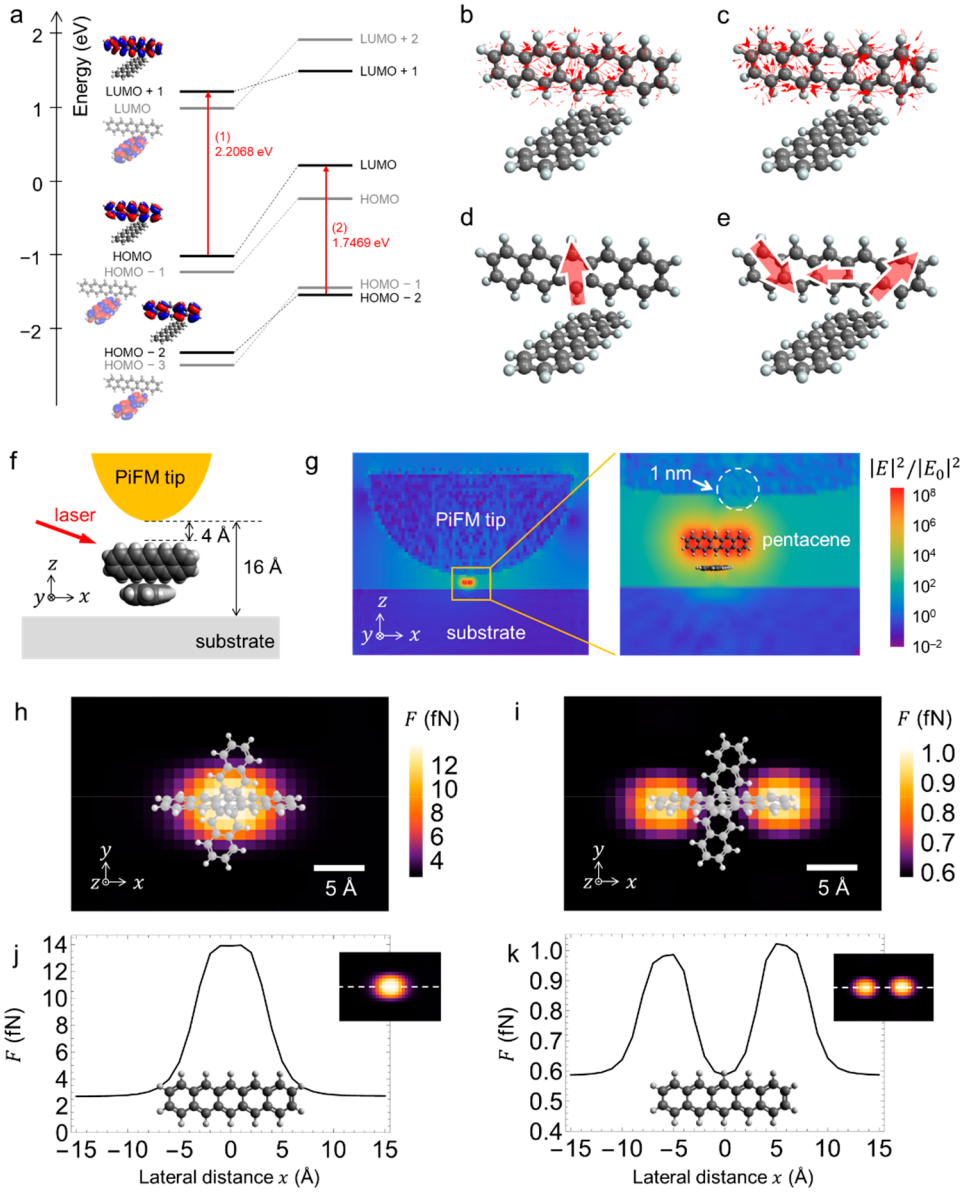

Figure 4. Quantum chemical calculations of the charge transfer in two pentacene molecules in an electrostatic field. (a) On the left, the orbitals and their energies in the absence of charge transfer and an electrostatic field; on the right, the energies considering divalent cationization and an electrostatic field. (b, c) Distribution of the dipole moments in discretized space for the first excitation transitions (1) and (2) in (a), respectively. (d, e) Schematic structure for (b) and (c), respectively. (f) Schematic picture of the calculation model. (g) Response electric field intensity maps of the PiFM measurement. (h, i) PiFM images of the pentacene molecules for transitions (1) and (2) in (a), respectively. (j, k) Line profiles of the photoinduced force along the axis of the molecule in the upper layer for the images shown in (h) and (i), respectively.

pentacene bilayer island. The topography in Figure 2a does not have a very high spatial resolution; therefore, the periodic arrangement of the upper molecules is difficult to observe. The CPD image in Figure 2b does not have any signs of the spatial resolution of a single molecule, meaning that there is no local CPD effect.[24] The PiFM image in Figure 2c has a much higher spatial resolution, and a periodic array of elongated bright spots can be observed. The periods of the elongated bright spots are 1.7 and 0.6 nm, which correspond to the lengths of the unit cell of the upper molecular array. The reason that the resolution of PiFM images is higher than that of CPD images is that the electrostatic force is inversely proportional to the square of the tip−sample distance (z), resulting in a wide interaction region,[19] while the photoinduced force is inversely proportional to the fourth power of z, resulting in a narrow interaction region (see Supplementary Notes 2 and 3). In PiFM, the interaction region is further narrowed owing to the localization effect of the picocavity, as explained later. In the PiFM image in Figure 2c, there are no artifacts because the electrostatic forces acting between the tip and the pentacene film are carefully removed and there is no molecular-scale CPD change between the tip and the pentacene film. Figure 2d shows an enlarged PiFM (Δf_{pif}) image of the region at the edge of the bilayer island indicated by the dotted square in Figure 2c. The elongated bright spots in Figure 2c are clearly split into two bright spots in Figure 2d. In addition, the bright spots (Δf_{pif} peaks) are paired inside the island but separate at the edge of the island (Figure 2e). Therefore, it is reasonable

https://doi.org/10.1021/acsnano.3c10924
ACS Nano 2024, 18, 1724−1732

that the bright spots (peaks of Δf_{pif}) correspond to the ends of the long axis direction of the pentacene molecules rather than to the center of the long axis direction of the pentacene molecules. The arrays of upper molecules in the identified pentacene bilayer are superimposed in Figure 2d. Thus, we succeeded in imaging the photoinduced forces acting inside of a single molecule.

We investigated the dependence of the van der Waals forces (F_{vdW}), the CPD, and the photoinduced forces (F_{pif}) on the tip−molecule distance (z) at the atomic scale. In Figures 3a, 3b, and 3c, we show the F_{vdW}−z, CPD−z, and F_{pif}−z curves of a single upper molecule of the pentacene bilayer, respectively. z = 0 is defined by the nearest tip−molecular distance, and the tip-molecule spacing at z = 0 is estimated to be 0.4 nm. Here, the light blue and red lines correspond to measurements at the edge and center of the molecule, respectively. There are no significant differences between the edge and center of the molecule with respect to F_{vdW} and CPD, but a difference is observed with respect to F_{pif}. As shown in Figure 3c, the F_{pif} values at the edge and the center are almost equal when z is larger than 0.3 nm, but differences begin to appear when z is smaller than 0.3 nm. The results in Figure 3c show that F_{pif} consists of the long-range photoinduced forces F_{fil} that reflect the macroscopic thin film properties of the pentacene bilayer and the short-range photoinduced forces F_{mol} that reflect the atomic-scale molecular properties of the pentacene bilayer (see Supplementary Notes 2 and 3 for the long-range photoinduced forces F_{fil} and the short-range photoinduced forces F_{mol}, respectively). In Figure 3c, the dashed line is the fitted long-range photoinduced force curve F_{fil}. The fitting was performed in the region of z > 0.3 nm. The dark blue and dark red lines correspond to the short-range photoinduced forces F_{mol} at the edge and center, respectively. In the region of z < 0.3 nm, the F_{mol} at the edge rapidly increases in attraction, while the F_{mol} at the center shows almost no attraction. These behaviors are reproduced by the theoretical simulation shown in Figure 3d, which is explained later.

Furthermore, we performed the 2D mapping of the photoinduced force along the long axis of a single upper molecule (Figure 3e) (Supplementary Note 11). Figures 3f and 3g show the results of the 2D mapping of the photoinduced force F_{pif} and the short-range photoinduced force F_{mol}, respectively. F_{mol} was obtained by subtracting the contribution of the fitted long-range photoinduced force F_{fil} from F_{pif}. Figure 3f clearly shows that the photoinduced force F_{pif} is slightly greater at the edge of the upper-layer molecules relative to the center, while Figure 3g shows that the short-range photoinduced force F_{mol} is larger near the edge of the upper-layer molecules. The short-range photoinduced force (attraction) increases near the edges when z is smaller than 0.3 nm but is almost zero at the center, even when z is less than 0.3 nm. This result suggests that light interacts strongly with the upper-layer molecules near the molecular edges. The spatial resolution of the short-range photoinduced force F_{mol} is approximately 0.6 nm. The magnitude of the short-range photoinduced force F_{mol} acting near the edge of a single molecule is very weak, less than 1 pN (Figure 3h) (see Supplementary Note 12 for the 2D mapping of the vector field of photoinduced forces).

We performed theoretical calculations of the PiFM images of the pentacene bilayer to investigate the cause of the contrast in the PiFM images (Supplementary Notes 13−17). In Figure 4a, we show the molecular orbitals and energy scheme obtained via quantum chemical calculations of the pentacene bilayer. In the calculation, we effectively incorporated the contribution from the CPD by applying an electrostatic field to the molecules to evaluate the charge transfer contribution. We further considered the effect of charge transfer to the substrate by assuming that the molecules are divalent cations (see Supplementary Note 13). In Figure 4a, the energies without and with consideration of CPD are shown on the left and right, respectively. In these calculations of electronic states, we consider the hybridization between the first and second molecular layers, although it is not strong. On the other hand, we confirmed that the hybridization with the neighboring molecules in the first and second layers is negligible and does not affect the present energy scheme. Therefore, the present simple model of the pentacene bilayer is sufficient for calculating PiFM images (Supplementary Note 18). The orbitals are localized in the upper or lower layer, and their energies are shown in black and gray. PiFM measurements are estimated to capture the optical properties of transitions between levels where electrons are localized in the upper layer, and transitions involving levels where electrons are localized in the lower layer can be negligible. Therefore, the respective first excitation transitions are shown by red arrows in Figures 4a (1) and (2), and the transition energies are 2.2068 and 1.7469 eV, respectively. Figures 4b and 4c show the distribution of the dipole moments for transitions (1) and (2) obtained from the wave function of the molecules in the discretized space with the extended discrete dipole approximation (e-DDA) method (see the Methods section), respectively. This polarization structure can be schematically understood, as shown in Figures 4d and 4e.

Figure 4g shows the response field map obtained by incorporating the polarization structure of the molecules into the e-DDA method by using the calculation model shown in Figure 4f. Here, we assume a 1 nm protrusion at the tip as the atomic-level surface structure of the tip surface. The observation of vibrational excitations of single molecules in surface-enhanced Raman spectroscopy has shown that a rigorous evaluation of optical mode volumes is possible with a resolution of a few angstroms.[25] It was shown by Benz et al. that these modes are due to the surface structures of the atoms at the tip, which naturally arise and are called picocavities. Also, molecular vibrations were directly observed by tip-enhanced Raman spectroscopy (TERS) owing to the localized field confined in picocavities.[26] The use of the TERS system as a precisely controllable junction in an ultrahigh-vacuum scanning tunneling microscope is shown to achieve ang-strom-scale resolution imaging, even at subatomic distances between the tip atoms and the molecules. Picocavities can occur in any geometry as long as the internal optical field is large enough to move a single atom from the surface.[27] The logic of resolution is the same for PiFM in that information on the localized field at the tip apex is acquired, and the theoretical analysis demonstrated the molecular resolution of PiFM owing to the presence of picocavities,[28,29] where the localized plasmon is enhanced in the nanogap between the tip and the substrate and molecules are strongly excited by the enhanced resonance light. We showed, in a previous work,[28] that the localized plasmon field of the nearest protrusion is strongly enhanced, even when there are multiple protrusions, which determine the image and resolution, at the tip. Thus, neighboring protrusions have little or no ghost-image-like

https://doi.org/10.1021/acsnano.3c10924
ACS Nano 2024, 18, 1724−1732

effect on the PiFM image; namely, the overall tip shape does not affect the image.

With the above-mentioned modeling, we obtained a PiFM image and a line profile of the photoinduced force, as shown in Figures 4h and 4j for transition (1) and Figures 4i and 4k for transition (2) in Figure 4a, by scanning the tip on the plane 0.4 nm above the upper-layer molecule. Without considering the contribution from the CPD, the PiFM image shows a strong signal at the center of the molecule. In contrast, with consideration of the contribution from the CPD, the PiFM image shows a strong signal at the edges of the molecule and a weak signal at the center. This is in good agreement with the experimental results in Figure 2d. The polarization of the induced localized plasmons radially spreads from the tip apex and can excite the dipole in the horizontal direction.[29] Considering the polarization structure of the molecule shown in Figure 4e, when the tip is at the edge of the molecule, the molecule can resonate with the plasmon, and the vertical components of the dipoles strengthen the induced force.[28−31] In contrast, when the tip is at the center of the molecule, these components of the dipoles inside the molecule cancel each other out, so no signal is observed. For the same situation as in Figure 4i, we demonstrate the F_{pif}−z curves at the edge and center of the pentacene in Figure 3d. For z = 0, the tip−molecule spacing is defined as 0.4 nm. As in Figure 3c, the light blue and red lines correspond to force curves at the edge and center of the molecule, respectively. In the calculations in Figure 3d, for reasons of model design, the contribution from the film F_{fil} is not determined. Instead, the dashed line plots the force contribution from the substrate as the background force. As in the experimental results, the magnitude of F_{mol} increases monotonically in attraction. The contrast in sensitivity at the edge and in the center was also reproduced. The orientation inferred from the obtained images in the experiments is consistent with that assumed in the simulations that well reproduce the measured PiFM images.

PiFM acquires images of the polarization structure corresponding to the resonance state of the molecule. The appearance of the images is considered to vary significantly for different excited states.[28] Theoretical calculations suggest that for incident light with an off-resonance frequency structures reflecting the internal polarizations of the molecule may not be observable. We theoretically demonstrate PiFM images with only the background dielectric constant in Supplementary Note 16. Although it is currently challenging to operate the existing PiFM system in a cryogenic environment under different frequency conditions, we are in the process of developing a system capable of operating at multiple frequencies for future studies.

As demonstrated above, the agreement between the calculation based on the present model and the experimental observations strongly suggests that the model with charge transfer from the second layer is plausible. The results in the present study prove that our PiFM system is a powerful tool to investigate near-field optical responses of single molecules, even with electronic structures strongly modulated by interactions with neighboring molecules and substrates.

CONCLUSION

In summary, using photoinduced force microscopy based on the heterodyne frequency modulation method and Kelvin probe force microscopy is a powerful method to investigate near-field optical responses of single molecules, even with electronic structures strongly modulated by interactions with neighboring molecules and substrates. The optical response inside a single pentacene molecule where charge transfer occurred was successfully observed with a spatial resolution of 0.6 nm, visualizing the multipolar excitation of a single molecule. The two-dimensional mapping of the photoinduced forces revealed that the signal is strong at the edges of the molecule and almost absent in the center. Theoretical calculations reveal that when charge transfer does not occur, the perpendicular components of the dipole are strongly excited at the center of the molecule, whereas when charge transfer occurs, the perpendicular components of the dipole are strongly excited at the edge of the molecule and cancel out at the center. This result is a real-space visualization of the optical response of a single molecule strongly affected by charge transfer, which could not be observed using conventional methods. These findings can only be achieved by combining microscopy techniques that simultaneously visualize the optical response of molecules and charge transfer between adjacent environments. Our approach and findings provide insights into designing molecular functions by considering the optical response at each step of layering molecules.

METHODS

Experimental Methods. All experiments were performed using a low-temperature ultrahigh-vacuum scanning probe microscope (Unisoku, USM 1400). The deflection of the cantilever was measured by an optical beam deflection method. An 830 nm laser diode and four segmented photodiodes were used to detect the cantilever deflection. A high-pass filter was used to avoid the influence of a 690 nm laser light on the deflection signal. The measurement was conducted at 3 × 10^{-11} Torr and 78 K.

The frequency modulation method was used to detect the tip−sample force interaction.[32] The oscillation frequency was maintained at the resonance frequency of the cantilever f_0, and the frequency shift of the resonance frequency Δf was measured by a phase-locked loop (PLL). The amplitude of the cantilever oscillation was kept constant by an amplitude gain controller (AGC). The topographies of the surface were obtained by using a z-feedback controller (Z-FBC) to keep Δf constant.

The heating effect by laser irradiation cannot be automatically excluded, even at low temperatures. The heterodyne FM method[13,20,21] was used to eliminate the apparent force due to the photothermal effect of light irradiation on the cantilever and tip and to measure only the photoinduced force between the tip and the sample surface (see Supplementary Note 5). The amplitude of the incident laser was modulated at a frequency of $2f_0 + f_{m1}$ (f_{m1} = 500 Hz), where f_0 is the resonance frequency of the cantilever and f_{m1} is set to be within the bandwidth of the PLL. The photoinduced force acting on the tip at a frequency of $2f_0 + f_{m1}$ was downconverted by the oscillating cantilever with a frequency of f_0; therefore, Δf was modulated at a frequency of f_{m1}. Δf modulated at a frequency of f_{m1} was detected by lock-in amplifier 1 (LIA1) as the photoinduced force coupled with the cantilever oscillation, which was denoted Δf_{pif}. The wavelength of the laser light was 690 nm, the power of the laser light was 7 mW, and the incidence angle of the light was 70° from the normal direction of the substrate.

FM−Kelvin probe force microscopy was used to compensate for the contact potential difference between the tip and the sample surface. The electrostatic force was modulated by applying an AC bias voltage V_{AC} with a frequency of f_{m2} that was lower than the cantilever resonance frequency and within the bandwidth of the PLL (V_{AC} = 0.3 V, f_{m2} = 1100 Hz). The electrostatic force modulated at a frequency of f_{m2} was detected by LIA2, and the CPD was obtained by using a Kelvin feedback controller (Kelvin-FBC) to make the electrostatic

https://doi.org/10.1021/acsnano.3c10924
ACS Nano 2024, 18, 1724−1732

force modulated at a frequency of f_{m2} zero (see Supplementary Note 6 for the electric circuit).

As the probe, a gold-coated cantilever with a spring constant of k = 40 N/m and a resonance frequency of f_0 = 300 kHz (Nanosensors: ATEC-NCAu) was used. The cantilever was oscillated with an amplitude A = 5 nm, and the frequency shift of the oscillating cantilever Δf was monitored. Since the heterodyne FM method was used, the signal from the photoinduced force became small when the cantilever vibration amplitude A was small, whereas when the cantilever vibration amplitude A was very large, the force became difficult to detect, and the signal from the photoinduced force became small. The cantilever oscillation amplitude with the best signal-to-noise ratio of the photoinduced force signal was A = 5 nm. The Ag (100) surface was cleaned by sputtering and annealing. Pentacene molecules were deposited on the Ag (100) surface, followed by postannealing of the substrate at 400 K for 5 min. As a result, pentacene bilayer islands were created on Ag (100) (see Supplementary Note 7 for the structure of the pentacene bilayer on Ag (100)). The acquisition time for the simultaneous measurement of topographic, CPD, and PiFM images was approximately 25 min.

The van der Waals forces (F_{vdW}) and the photoinduced forces (F_{pif}) depending on the tip−molecule distance (z) were calculated from the Δf−z curves[33] and Δf_{pif}−z curves,[13] respectively, where z = 0 is defined as the nearest tip−molecule distance.

Theoretical Calculation Methods. We performed theoretical calculations on the PiFM images of the pentacene bilayer. We used the e-DDA method[28,34] to self-consistently obtain the total response electric field induced by the polarization of the molecule.[29] In this method, the whole space was divided into small cells of volume V, and each cell was treated as a dipole. Considering the time-harmonic electric field, to obtain the response field, we solved the following equation:[35,36]

$$\boldsymbol{E}(\boldsymbol{r}_i, \omega) = \boldsymbol{E}_0(\boldsymbol{r}_i, \omega) + \sum_j V\boldsymbol{G}(\boldsymbol{r}_i, \boldsymbol{r}_j, \omega)\boldsymbol{P}(\boldsymbol{r}_j, \omega) \tag{1}$$

where the coordinate $\boldsymbol{r}_i$ represents the position of each divided cell. $\mathbf{E}(\mathbf{r},\omega)$ and $\boldsymbol{E}_0(\mathbf{r},\omega)$ are the total response electric field and incident electric field with an angular frequency ω, respectively. $\boldsymbol{G}(\mathbf{r},\mathbf{r}',\omega)$ is Green's function in free space. $\mathbf{P}(\mathbf{r},\omega)$ is the polarization defined by the susceptibility of the materials as follows:

$$\boldsymbol{P}(\boldsymbol{r}_i, \omega) = \begin{cases} \chi_{\mathrm{met}}(\boldsymbol{r}_i, \omega)\boldsymbol{E}(\boldsymbol{r}_i, \omega), \\ \sum_j V\chi_{\mathrm{mol}}(\boldsymbol{r}_i, \boldsymbol{r}_j, \omega)\boldsymbol{E}(\boldsymbol{r}_j, \omega) \end{cases} \tag{2}$$

where $\chi_{\mathrm{met}}(\mathbf{r},\omega)$ is the susceptibility of the metal structures relative to the tip and substrate defined by the Drude-critical points model.[37] $\chi_{\mathrm{mol}}(\mathbf{r},\omega)$ is the nonlocal susceptibility[29] obtained from the wave function of the molecule under the first-order perturbation approximation:

$$\chi_{\mathrm{mol}}(\boldsymbol{r}_i, \boldsymbol{r}_j, \omega) = \sum_n \sum_{n'} \frac{1}{V} \frac{d^*_{n,n'}(\boldsymbol{r}_i) d_{n,n'}(\boldsymbol{r}_j)}{\hbar\omega_{n,n'} - \hbar\omega - i\gamma_{\mathrm{mol}}} \tag{3}$$

where γ_{mol} is the decay rate and $d_{n,n'(r)}$ is the dipole moment with energy $\hbar\omega_{n,n'}$ corresponding to the transition from the n-th state to the n'-th state. The dipole moment was determined by the wave function of the molecule: $d_{n,n'(r)} = \phi^*_{n'}(\boldsymbol{r})\, e\boldsymbol{r}\phi_n(\boldsymbol{r})$. In this study, we used GAMESS(US)[38] to obtain the wave functions $\phi_n(\mathbf{r})$ and energies of the molecule. In this calculation, we evaluated the photoinduced force acting on the tip. The force can be expressed by time averaging the Lorentz force as in the following formula:[39]

$$\boldsymbol{F}(\omega) = \frac{1}{2}\mathrm{Re}\left[\sum_i V(\nabla \boldsymbol{E}^*(\boldsymbol{r}_i, \omega))\cdot\boldsymbol{P}(\boldsymbol{r}_i, \omega)\right] \tag{4}$$

where the summation is performed over the cells that configure the tip.

ASSOCIATED CONTENT

Supporting Information

The Supporting Information is available free of charge at https://pubs.acs.org/doi/10.1021/acsnano.3c10924.

General theory of the photoinduced force between a tip and a sample; photoinduced force between a tip and a thin film on the substrate; photoinduced force of submolecular resolution; photoinduced force acting on the tip; heterodyne-FM configuration for the measurement of photoinduced force; electric circuit of PiFM; structure of the pentacene bilayer on Ag (100); tilted incident light and photoinduced force enhancement at the left edge of the bilayer islands; influence of the electrostatic force on photoinduced force mapping; influence of photovoltage on the photoinduced force measurement; 2D mapping of the forces; vector field of the photoinduced force above pentacene single molecule; electronic states of a pentacene bilayer on a metal substrate; PiFM image of pentacene monolayer; theoretical considerations on the magnitude of force; PiFM image with off-resonant light; quenching effect of molecules near metallic materials; absence of orbital hybridization between adjacent molecules (PDF)

AUTHOR INFORMATION

Corresponding Authors

Hajime Ishihara − *Department of Materials Engineering Science, Osaka University, Toyonaka, Osaka 560-8531, Japan;* orcid.org/0000-0001-6074-4579; Email: ishi@mp.es.osaka-u.ac.jp

Yasuhiro Sugawara − *Department of Applied Physics, Osaka University, Suita, Osaka 565-0871, Japan;* orcid.org/0000-0002-1233-5313; Email: sugawara@ap.eng.osaka-u.ac.jp

Authors

Tatsuya Yamamoto − *Department of Applied Physics, Osaka University, Suita, Osaka 565-0871, Japan*

Hidemasa Yamane − *Department of Physics, Kitasato University, Sagamihara, Kanagawa 252-0373, Japan; Osaka Research Institute of Industrial Science and Technology, Izumi, Osaka 594-1157, Japan;* orcid.org/0000-0001-8720-5348

Nobuhiko Yokoshi − *Department of Physics and Electronics, Osaka Metropolitan University, Sakai, Osaka 599-8531, Japan;* orcid.org/0000-0003-2949-5943

Hisaki Oka − *Department of Physics, Kitasato University, Sagamihara, Kanagawa 252-0373, Japan;* orcid.org/0000-0003-4532-3949

Complete contact information is available at: https://pubs.acs.org/10.1021/acsnano.3c10924

Author Contributions

T. Yamamoto. and Y. Sugawara performed the high-precision PiFM measurements. H. Yamane, N. Yokoshi, H. Oka, and H. Ishihara performed the numerical calculations.

Notes

The authors declare no competing financial interest.

ACKNOWLEDGMENTS

This work was supported by JSPS KAKENHI Grant Numbers JP16H06504, JP16H06507, JP16J00304, JP21H04662,

JP21H05019, JP21K14554, JP22H05132, JP22K18946, and JP22K18970.

REFERENCES

(1) Zhang, L.; Yang, C.; Lu, C.; Li, X.; Guo, Y.; Zhang, J.; Lin, J.; Li, Z.; Jia, C.; Yang, J.; Houk, K. N.; Mo, F.; Guo, X. Precise electrical gating of the single-molecule Mizoroki-Heck reaction. *Nat. Commun.* **2022**, *13*, 4552.
(2) Engwerda, A. H. J.; Fletcher, S. P. A molecular assembler that produces polymers. *Nat. Commun.* **2020**, *11*, 4156.
(3) Fedyuk, V.; Erez, N.; Furth, N.; Beresh, O.; Andreishcheva, E.; Shinde, A.; Jones, D.; Zakai, B. B.; Mavor, Y.; Peretz, T.; Hubert, A.; Cohen, J. E.; Salah, A.; Temper, M.; Grinshpun, A.; Maoz, M.; Zick, A.; Ron, G.; Shema, E. Multiplexed, single-molecule, epigenetic analysis of plasma-isolated nucleosomes for cancer diagnostics. *Nat. Biotechnol.* **2023**, *41*, 212−218.
(4) Berger, J.; Ondráček, M.; Stetsovych, O.; Malý, P.; Holý, P.; Rybáček, J.; Švec, M.; Stará, I. G.; Mančal, T.; Starý, I.; Jelínek, P. Quantum dissipation driven by electron transfer within a single molecule investigated with atomic force microscopy. *Nat. Commun.* **2020**, *11*, 1337.
(5) Cao, S.; Rosławska, A.; Doppagne, B.; Romeo, M.; Feron, M.; Cherioux, F.; Bulou, H.; Scheurer, F.; Schull, G. Energy funnelling within multichromophore architectures monitored with subnanometre resolution. *Nat. Chem.* **2021**, *13*, 766−770.
(6) Chen, C.; Chu, P.; Bobisch, C. A.; Mills, D. L.; Ho, W. Viewing the interior of a single molecule: vibronically resolved photon imaging at submolecular resolution. *Phys. Rev. Lett.* **2010**, *105*, No. 217402.
(7) Lee, J.; Kevin, J.; Crampton, T.; Tallarida, N.; Apkarian, V. A. Visualizing vibrational normal modes of a single molecule with atomically confined light. *Nature* **2019**, *568*, 78−82.
(8) Kong, F. F.; Tian, X. J.; Zhang, Y.; Yu, Y. J.; Jing, S. H.; Zhang, Y.; Tian, G. J.; Luo, Y.; Yang, J. Y.; Dong, Z. C.; Hou, J. G. Probing intramolecular vibronic coupling through vibronic-state imaging. *Nat. Commun.* **2021**, *12*, 1280.
(9) Yang, B.; Chen, G.; Ghafoor, A.; Zhang, Y.; Zhang, Y.; Zhang, Y.; Luo, Y.; Yang, J.; Sandoghdar, V.; Aizpurua, J.; Dong, Z.; Hou, J. G. Sub-nanometre resolution in single-molecule photoluminescence imaging. *Nat. Photonics* **2020**, *14*, 693−699.
(10) Rosławska, A.; Neuman, T.; Doppagne, B.; Borisov, A. G.; Romeo, M.; Scheurer, F.; Aizpurua, J.; Schull, G. Mapping Lamb, Stark, and Purcell effects at a chromophore-picocavity junction with hyper-resolved fluorescence microscopy. *Phys. Rev. X* **2020**, *12*, No. 011012.
(11) Rajapaksa, I.; Uenal, K.; Wickramasinghe, H. K. Image force microscopy of molecular resonance: A microscope principle. *Appl. Phys. Lett.* **2010**, *97*, No. 173121.
(12) Jahng, J.; Brocious, J.; Fishman, D. A.; Huang, F.; Li, X.; Tamma, V. A.; Wickramasinghe, H. K.; Potma, E. O. Gradient and scattering forces in photoinduced force microscopy. *Phys. Rev. B* **2014**, *90*, No. 155417.
(13) Yamanishi, J.; Yamane, H.; Naitoh, Y.; Li, Y. J.; Yokoshi, N.; Kameyama, T.; Koyama, S.; Torimoto, T.; Ishihara, H.; Sugawara, Y. Optical force mapping at the single-nanometre scale. *Nat. Commun.* **2021**, *12*, 3865.
(14) Yamanishi, J.; Li, Y. J.; Naitoh, Y.; Sugawara, Y. Nanoscale optical imaging with photoinduced force microscopy in heterodyne amplitude modulation and heterodyne frequency modulation modes. *J. Photochem. Photobiol. C Photochem. Rev.* **2020**, *52*, No. 100532.
(15) Jahng, J.; Fishman, D. A.; Park, S.; Nowak, D. B.; Morrison, W. A.; Wickramasinghe, H. K.; Potma, E. O. Linear and Nonlinear Optical Spectroscopy at the Nanoscale with Photoinduced Force Microscopy. *Acc. Chem. Res.* **2015**, *48*, 2671−2679.
(16) Tamma, V. A.; Beecher, L. M.; Shumaker-Parry, J. S.; Wickramasinghe, H. K. Detecting stimulated Raman responses of molecules in plasmonic gap using photon induced forces. *Opt. Express* **2018**, *26*, 31439.
(17) Almajhadi, M. A.; Uddin, S. M. A.; Wickramasinghe, H. K. Observation of nanoscale opto-mechanical molecular damping as the origin of spectroscopic contrast in photo induced force microscopy. *Nat. Commun.* **2020**, *11*, 5691.
(18) Nonnenmacher, M.; O'Boyle, M. P.; Wickramasinghe, H. K. Kelvin probe force microscopy. *Appl. Phys. Lett.* **1991**, *58*, 2921−2923.
(19) Sadewasser, S.; Glatzel, T. (Eds.). *Kelvin Probe Force Microscopy: From Single Charge Detection to Device Characterization*, 2018, *65*, Springer.
(20) Yamanishi, J.; Naitoh, Y.; Li, Y. J.; Sugawara, Y. Heterodyne technique in photoinduced force microscopy with photothermal effect. *Appl. Phys. Lett.* **2017**, *110*, No. 123102.
(21) Yamanishi, J.; Naitoh, Y.; Li, Y. J.; Sugawara, Y. Heterodyne Frequency Modulation in Photoinduced Force Microscopy. *Phys. Rev. Appl.* **2018**, *9*, No. 024031.
(22) Rockey, T. J.; Wilhelm, M. J.; Dai, H. L. Ultrathin films of pentacene on Ag(111): Charge-transfer bonding and interadsorbate interactions. *J. Phys. Chem. C* **2021**, *125*, 3385−3395.
(23) Jaeckel, B.; Sambur, J. B.; Parkinson, B. A. The influence of metal work function on the barrier heights of metal/pentacene junctions. *J. Appl. Phys.* **2008**, *103*, No. 063719.
(24) Sadewasser, S.; Jelinek, P.; Fang, C.; Custance, O.; Yamada, Y.; Sugimoto, Y.; Abe, M.; Morita, S. New insights on atomic-resolution frequency-modulation Kelvin-probe force-microscopy imaging of semiconductors. *Phys. Rev. Lett.* **2009**, *103*, 5−8.
(25) Benz, F.; Schmidt, M. K.; Dreismann, A.; Chikkaraddy, R.; Zhang, Y.; Demetriadou, A.; Carnegie, C.; Ohadi, H.; De Nijs, B.; Esteban, R.; Aizpurua, J.; Baumberg, J. J. Single-molecule optomechanics in "picocavities". *Science* **2016**, *354*, 726−729.
(26) Lee, J.; Crampton, K. T.; Tallarida, N.; Ara Apkarian, V. Visualizing vibrational normal modes of a single molecule with atomically confined light. *Nature* **2019**, *568*, 78−82.
(27) Baumberg, J. J. Picocavities: a Primer. *Nano Lett.* **2022**, *22*, 5859−5865.
(28) Yamane, H.; Yokoshi, N.; Ishihara, H. High-resolution measurement of molecular internal polarization structure by photo-induced force microscopy. *Appl. Sci.* **2021**, *11*, 6937.
(29) Yamane, H.; Yokoshi, N.; Oka, H.; Sugawara, Y.; Ishihara, H. Near-field circular dichroism of single molecules. *Opt. Express* **2023**, *31*, 3415−3426.
(30) Imada, H.; Miwa, K.; Imai-Imada, M.; Kawahara, S.; Kimura, K.; Kim, Y. Single-Molecule Investigation of Energy Dynamics in a Coupled Plasmon-Exciton System. *Phys. Rev. Lett.* **2017**, *119*, No. 013901.
(31) Yamane, H.; Yamanishi, J.; Yokoshi, N.; Sugawara, Y.; Ishihara, H. Theoretical analysis of optically selective imaging in photoinduced force microscopy. *Opt. Exp.* **2020**, *28*, 34787−34803.
(32) Albrecht, T. R.; Grütter, P.; Horne, D.; Rugar, D. Frequency modulation detection using high-Q cantilevers for enhanced force microscope sensitivity. *J. Appl. Phys.* **1991**, *69*, 668−673.
(33) Sader, J. E.; Jarvis, S. P. Accurate formulas for interaction force and energy in frequency modulation force spectroscopy. *Appl. Phys. Lett.* **2004**, *84*, 1801−1803.
(34) Takase, M.; Ajiki, H.; Mizumoto, Y.; Komeda, K.; Nara, M.; Nabika, H.; Yasuda, S.; Ishihara, H.; Murakoshi, K. Selection-rule breakdown in plasmon-induced electronic excitation of an isolated single-walled carbon nanotube. *Nature Photo.* **2013**, *7*, 550−554.
(35) Purcell, E. M.; Pennypacker, C. R. Scattering and Absorption of Light by Nonspherical Dielectric Grains. *Astrophys. J.* **1973**, *186*, 705−714.
(36) Livesay, D. E.; Chen, K. M. Electromagnetic Fields Induced Inside Arbitrarily Shaped Biological Bodies. *IEEE Transaction on Microwave Theory Techniques* **1974**, *22*, 1273−1280.
(37) Vial, A.; Laroche, T. Comparison of gold and silver dispersion laws suitable for FDTD simulations. *Appl. Phys. B: Laser Opt.* **2008**, *93*, 139−143.
(38) Schmidt, M. W.; Baldridge, K. K.; Boatz, J. A.; Elbert, S. T.; Gordon, M. S.; Jensen, J. H.; Koseki, S.; Matsunaga, N.; Nguyen, K. A.; Su, S.; Windus, T. L.; et al. General atomic and molecular electronic structure system. *J. Comput. Chem.* **1993**, *14*, 1347−1963.

https://doi.org/10.1021/acsnano.3c10924
ACS Nano 2024, 18, 1724−1732

(39) Iida, T.; Ishihara, H. Theory of resonant radiation force exerted on nanostructures by optical excitation of their quantum states: From microscopic to macroscopic descriptions. *Phys. Rev. B* **2008**, *77*, 245319.

https://doi.org/10.1021/acsnano.3c10924
ACS Nano 2024, 18, 1724−1732